PRAMANA
— journal of
physics

© Indian Academy of Sciences

Vol. 69, No. 4
October 2007
pp. 603–616

Surface segregation of the metal impurity to the (1 0 0) surface of fcc metals

JIAN-MIN ZHANG[1], BO WANG[1] and KE-WEI XU[2]
[1]College of Physics and Information Technology, Shaanxi Normal University, Xian 710062, Shaanxi, People's Republic of China
[2]State-Key Laboratory for Mechanical Behavior of Materials, Xian Jiaotong University, Xian 710049, Shaanxi, People's Republic China
E-mail: jianm_zhang@yahoo.com

MS received 10 December 2006; revised 19 June 2007; accepted 5 July 2007

Abstract. The surface segregation energies for a single metal impurity to the (1 0 0) surface of nine fcc metals (Cu, Ag, Au, Ni, Pd, Pt, Rh, Al and Ir) have been calculated using the MAEAM and molecular dynamics (MD) simulation. The results show that the effect of the surface is down to the fourth-layer and an oscillatory or monotonic damping ($|E_1| > |E_2| > |E_3| > |E_4|$) phenomenon in segregation energy has been obtained. The absolute value of the segregation energy E_1 for a single impurity in the first atomic layer is much higher than that in the nether layers. Thus, whether the surface segregation will work or not is mainly determined by E_1 which is in good relation to the differences in surface energy between the impurity and host crystals $\Delta Q = Q_{\mathrm{imp}} - Q_{\mathrm{hos}}$. So we conclude that an impurity with lower surface energy will segregate to the surface of the host with higher surface energy.

Keywords. Fcc metals; surface segregation; modified analytic embedded-atom method and surface energy.

PACS Nos 61.30.Hn; 68.47.De; 82.45.Jn

1. Introduction

The equilibrium compositions of the first few surface atom layers which differ from the bulk ones in alloys is known as surface segregation phenomena. It plays a very important role in many surface-related applications, such as corrosion, oxidation, catalysis, tribology, epitaxial growth, morphology [1,2] and so on. With the fast development of modern science and technology, many surface analytic techniques, low-energy electron diffraction (LEED) [3], low-energy ion scattering (LEIS) [4], Auger electron spectroscopy (AES) [5], atom-probe field ion microscopy (AP-FIM) [6] etc., have been used to measure the surface chemical compositions of alloys and compounds. In addition, many theoretical approaches, the first-principles [7], density functional theory [8], Miedema theory [9,10], tight-binding approximation

[11–13], pair-potential theory [14,15], quasi-atom theory [16] and effective-medium theory [17] etc., have also been used to investigate the surface compositions and structures.

In this paper, the surface segregation energy for a single metal impurity to the (1 0 0) surface of nine fcc metals (Cu, Ag, Au, Ni, Pd, Pt, Rh, Al and Ir) has been calculated using the modified analytic embedded-atom method (MAEAM). The lattice relaxation is treated with the molecular dynamics (MD) simulation at a temperature of absolute zero and constant volume. The results show that the effect of the surface is down to the fourth-layer and an oscillatory or monotonic damping ($|E_1| > |E_2| > |E_3| > |E_4|$) phenomenon in segregation energy has been obtained. The absolute value of the segregation energy E_1 for a single impurity in the first atomic layer is much higher than that in the nether layers. Thus, whether the surface segregation will work or not is mainly determined by E_1 which is in good relation to the differences in surface energy between the impurity and host crystals $\Delta Q = Q_{\text{imp}} - Q_{\text{hos}}$. So we conclude that an impurity with lower surface energy will segregate to the surface of the host with higher surface energy.

The MAEAM was chosen because it is reasonably good in constructing the interatomic potentials for doped solid solution or alloy systems. In the embedded-atom method (EAM) originally proposed by Daw and Baskes [18,19], the embedded energy and pair potential are not given in analytical forms and do not consider the directional bonding of the atoms in a crystal. Thus EAM have no universality and they are very difficult to be applied systematically to doped solid solutions or alloys [20], and hence only very limited properties of alloys are available in the alloy systems. Thus, in order to construct one potential for doped solid solutions or alloy systems, Johnson provided an analytic EAM (AEAM) for fcc, bcc and hcp metals [21–23]. Following AEAM, Zhang *et al* [24] developed MAEAM by adding an energy modification term corresponding to a linear superposition of spherically averaged atomic electron density. This method seemed advisable to employ rather than the EAM for the calculations of doped solid solution and alloy, e.g. the elastic constants C_{11}, C_{12} and C_{44} of Ni_3Al calculated are 1197, 792 and 604 [25] by MAEAM, and 1572, 855 and 786 [26] by EAM. However, their experimental values are 1260, 790 and 736 eV·nm^{-3} [27]. In our previous papers [28–32], the MAEAM was employed successfully to investigate the interface, grain boundary, surface adsorption and point defects.

2. Methodology

2.1 *MAEAM*

In MAEAM, the total energy of a system E_{t} is expressed as [24]

$$E_{\text{t}} = \sum_i F(\rho_i) + \frac{1}{2}\sum_i \sum_{j(\neq i)} \phi(r_{ij}) + \sum_i M(P_i), \tag{1}$$

$$\rho_i = \sum_{j(\neq i)} f(r_{ij}), \tag{2}$$

$$P_i = \sum_{j(\neq i)} f^2(r_{ij}), \tag{3}$$

where $F(\rho_i)$ is the energy to embed an atom in site i with electron density ρ_i, which is given by a linear superposition of the spherical averaged atomic electron density of other atoms $f(r_{ij})$, r_{ij} is the separation distance of atom j from atom i, $\phi(r_{ij})$ is the pair potential between atoms i and j, and $M(P_i)$ is the modified term, which describes the energy change due to the non-spherical distribution of atomic electronic density and deviation from the linear superposition. Embedding function $F(\rho_i)$, pair potential $\phi(r_{ij})$, modified term $M(P_i)$, and atomic electron density $f(r_{ij})$ take the following forms [33,34]:

$$F(\rho_i) = -F_0 \left[1 - n \ln\left(\frac{\rho_i}{\rho_e}\right)\right] \left(\frac{\rho_i}{\rho_e}\right)^n, \tag{4}$$

$$\phi(r_{ij}) = k_0 + k_1 \left(\frac{r_{ij}}{r_{1e}}\right)^2 + k_2 \left(\frac{r_{ij}}{r_{1e}}\right)^4 + k_3 \left(\frac{r_{1e}}{r_{ij}}\right)^{12}, \quad r_{ij} \leq r_{2e}, \tag{5}$$

$$M(P_i) = \alpha \left(\frac{P_i}{P_e} - 1\right)^2 \exp\left[-\left(\frac{P_i}{P_e} - 1\right)^2\right], \tag{6}$$

$$f(r_{ij}) = f_e \left(\frac{r_{1e}}{r_{ij}}\right)^6, \tag{7}$$

where the subscript e denotes equilibrium state and r_{1e} is the first nearest neighbor distance at equilibrium. In this paper, the atomic electron density at equilibrium state f_e is chosen as [34]

$$f_e = \left(\frac{E_\mathrm{c} - E_\mathrm{1f}}{\Omega}\right)^{3/5}, \tag{8}$$

where $\Omega = a^3/4$ is the atomic volume in a metal with fcc structure.

The seven parameters n, α, F_0, k_0, k_1, k_2 and k_3 in eqs (4)–(6) can be determined by fitting the cohesion energy E_c, the mono-vacancy formation energy E_1f given by $E_\mathrm{1f} = E_\mathrm{t}^v - (E_\mathrm{t} - E_\mathrm{c})$, where E_t^v and E_t are the total energies of the lattices with and without a vacancy and E_c is the cohesion energy and compensates for the missing atom, the lattice constant a, and elastic constants C_{11}, C_{12} and C_{44}. According to the principle that the energy versus separation distance curve fits the Rose equation [35], we get

$$n = \sqrt{\frac{\Omega(C_{11} + 2C_{12})(C_{11} - C_{12})}{(216 E_\mathrm{1f} C_{44})}}, \tag{9}$$

$$\alpha = \frac{\Omega(C_{12} - C_{44})}{32} - \frac{n^2 F_0}{8}, \tag{10}$$

$$F_0 = E_{\rm c} - E_{1\rm f}. \tag{11}$$

The parameters of the potential energy k_0, k_1, k_2 and k_3 can be calculated with the following formulae [34]:

$$k_0 = -\frac{E_{1\rm f}}{9} - \frac{\Omega(-2989C_{11} + 2989C_{12} + 5481C_{44})}{42840}, \tag{12}$$

$$k_1 = \frac{\Omega(-939C_{11} + 939C_{12} + 1311C_{44})}{9520}, \tag{13}$$

$$k_2 = \frac{\Omega(32C_{11} - 32C_{12} - 33C_{44})}{1020}, \tag{14}$$

$$k_3 = \frac{8\Omega(-C_{11} + C_{12} + 9C_{44})}{5355}. \tag{15}$$

According to the analysis of Zhang *et al*, the pair-potential $\phi(r_{ij})$ represented by eq. (5) is available only for the separated distance between atoms, is shorter than the second neighbor distance r_{2e} and should be substituted by following cubic spline function (termed as a cut-off potential) while the separated distance between atoms varies in the range r_{2e} to $r_{\rm c}$ [33]:

$$\phi(r_{ij}) = l_0 + l_1\left(\frac{r_{ij}}{r_{2e}} - 1\right) + l_2\left(\frac{r_{ij}}{r_{2e}} - 1\right)^2 + l_3\left(\frac{r_{ij}}{r_{2e}} - 1\right)^3, \quad r_{2e} < r_{ij} \le r_{\rm c}. \tag{16}$$

Four parameters l_0, l_1, l_2, l_3 and cut-off radius $r_{\rm c}$ are taken as

$$l_0 = k_0 + k_1 s^2 + k_2 s^4 + k_3 s^{-12}, \tag{17}$$

$$l_1 = 2k_1 s^2 + 4k_2 s^4 - 12k_3 s^{-12}, \tag{18}$$

$$l_2 = -\frac{2l_1}{(\gamma - 1)} - \frac{3l_0}{(\gamma - 1)^2}, \tag{19}$$

$$l_3 = \frac{l_1}{(\gamma - 1)^2} + \frac{2l_0}{(\gamma - 1)^3}, \tag{20}$$

$$r_{\rm c} = r_{2e} + 0.75(r_{3e} - r_{2e}), \tag{21}$$

where r_{2e} and r_{3e} are the second and third neighbor distance at equilibrium, $s = r_{2e}/r_{1e}$ and $\gamma = r_{\rm c}/r_{2e}$, respectively.

Table 1. The input physical parameters for nine fcc metals [36–39].

Metal	a (Å)	E_c (eV)	E_{1f} (eV)	C_{11} (eV·nm^{-3})	C_{12} (eV·nm^{-3})	C_{44} (eV·nm^{-3})
Cu	3.6147	3.49	1.17	1050	760	470
Ag	4.0857	2.95	1.10	770	570	280
Au	4.0788	3.81	0.90	1190	1010	260
Ni	3.5236	4.44	1.45	1540	960	760
Pd	3.8907	3.89	1.30	1400	1080	450
Pt	3.9239	5.84	1.20	2120	1720	520
Rh	3.8401	5.75	2.90	2470	1450	1380
Al	4.0496	3.39	0.64	650	460	270
Ir	3.8389	6.94	3.50	3550	1940	2060

The input physical parameters are listed in table 1, and the calculated model parameters f_e, n, α, F_0, k_i and l_i ($i = 0, 1, 2, 3$) for nine fcc metals Cu, Ag, Au, Ni, Pd, Pt, Rh, Al and Ir are listed in table 2 for convenience.

In the present paper, the alloy interaction potential between different atomic species is that of Johnson with some modification, as follows [40]:

$$\phi^{AB}(r) = \frac{1}{2}\left[\frac{\Omega^B f^B(r)}{\Omega^A f^A(r)}\phi^A(r) + \frac{\Omega^A f^A(r)}{\Omega^B f^B(r)}\phi^B(r)\right], \tag{22}$$

here the superscripts A and B in the atomic volume Ω, electron density function $f(r)$ and interactive potential $\phi(r)$ represent atoms A and B respectively.

2.2 *Computational procedure*

The total number of atoms is 1445 and that of the atoms on each layer is 85, a surface super-cell containing 17 layers of (1 0 0) atomic plane from the bottom of the cell along the x-axis are used for each fcc metal, which is large enough to model the surface interaction and effects between the host and impurity atoms. A mantle of the atoms fixed at their perfect lattice positions around the super-cell is used as boundary to ensure that each atom in the super-cell has a complete set of neighbors within the range of interatomic potential except for introduction of the surface. The lattice relaxation that resulted from the existence of the interaction between the host and impurity atoms are treated with the MD simulation [33,34]. The force applied to the ith atom from the other atoms is calculated by

$$f_i^\alpha = -\frac{\partial E_i}{\partial r_{ij}^\alpha} = -\left[F'(\rho_i)\sum_{j(\neq i)} f'(r_{ij})\frac{r_{ij}^\alpha}{r_{ij}} + \frac{1}{2}\sum_{j(\neq i)}\phi'(r_{ij})\frac{r_{ij}^\alpha}{r_{ij}} + 2M'(P_i)\sum_{j(\neq i)} f(r_{ij})f'(r_{ij})\frac{r_{ij}^\alpha}{r_{ij}}\right], \tag{23}$$

where the superscript α (denoted by x, y or z) in f_i^α and r_{ij}^α represents the αth component of the force (f_i) and the separation distance (r_{ij}) of atom j from

Table 2. MAEAM model parameters for nine fcc metals, α, F_0, k_i and l_i ($i = 0, 1, 2, 3$). The values are in eV.

Metal	f_e	n	α	F_0	k_0	k_1	k_2	k_3	l_0	l_1	l_2	l_3
Cu	0.3767	0.2722	0.0855	2.3200	−0.6011	0.4265	−0.0721	0.0695	−0.0355	0.5390	−2.6446	4.1359
Ag	0.2638	0.3129	0.1319	1.8500	−0.4951	0.3211	−0.0475	0.0591	−0.0419	0.5137	−1.6724	0.5876
Au	0.3472	0.4404	0.3271	2.9100	−0.4517	0.3062	−0.0469	0.0547	−0.0256	0.4642	−2.8060	5.6523
Ni	0.4593	0.3037	0.0339	2.9900	−0.7820	0.5190	−0.0699	0.1023	−0.0221	0.9382	−8.8013	23.8030
Pd	0.3525	0.3643	0.2469	2.5900	−0.6634	0.4477	−0.0665	0.0820	−0.0329	0.7107	−4.9574	11.2690
Pt	0.4926	0.4992	0.4219	4.6400	−0.7167	0.4857	−0.0646	0.0966	−0.0021	0.8916	−10.3630	30.5250
Rh	0.3822	0.2995	−0.0009	2.8500	−1.8142	1.2661	−0.1790	0.2411	0.0055	2.1545	−26.1470	78.1380
Al	0.3400	0.3643	0.0530	2.7500	−0.4245	0.3062	−0.0461	0.0556	0.0044	0.4772	−6.1288	18.6410
Ir	0.4282	0.3296	−0.0998	3.4400	−2.5278	1.7663	−0.2282	0.3577	0.0974	3.3462	−49.9870	158.4500

atom i. $E_i = F(\rho_i) + \frac{1}{2}\sum_{j(\neq i)} \phi(r_{ij}) + M(P_i)$ is the energy contribution from atom i and eq. (1) becomes

$$E_{\mathrm{t}} = \sum_i E_i. \tag{24}$$

3. Results and discussion

The simulation is done for some time under zero temperature and zero pressure for equilibration purposes, because the computation simulation technique we employ does not explicitly account for the effect of temperature, and the corresponding results are strictly consistent with 0 K data. In order to assess the stability of the impurity in different sites of the crystallite, we simulate the energy for an impurity atom in different non-equivalent impurity positions of nine fcc metal (1 0 0) surfaces based on the energy minimization principle. The resulting equilibrated configuration is mapped onto its corresponding local minimum-energy configuration by simulation. In all calculations a sufficient number of atoms around the mobile impurity are treated as movable discrete particles. The calculation treats the distortion of the lattice far from impurity as the superposition of displacement fields of point forces in the elastic continuum. The electronic contributions to the relaxation of the lattice due to the redistribution of the electrons are neglected. The lattice distortion in the vicinity of the impurity is determined by an iteration process minimizing the energy: at each step one calculates the displacements of the atoms from the 'equilibrium positions' given in the previous step; in this way rapid convergence is attained. In all cases the impurity produces a displacement of the host atoms surrounding it, and during relaxation of the lattice the impurity migrates from an arbitrarily chosen position into an equilibrium configuration. The stability of the various configurations versus different impurity sites is beyond the scope of this work, and we have just observed the most stable and relatively immobile surface segregation configurations.

For the extreme dilute limits of the alloy, a single impurity in a lattice point can be assumed to be created by substituting a host atom from the corresponding position. The surface segregation energy E, which is defined as the difference in energy for placing a substitutional impurity or solute atom at different surface atomic layers of an otherwise pure material relative to placing the substitutional impurity in the bulk, is calculated for a single impurity placed in each atomic plane of the nine fcc metal (1 0 0) surfaces.

The results show that the effect of the surface to the segregation energy is only down to the fourth-layer. So they are listed in table 3 (top lines) together with other available theoretical and experimental values for comparing, and the more accurate first principle values [67,68] are listed in the last lines of table 3. From energy minimization and definition of the surface segregation energy above, we know that a negative value of a surface segregation energy E on an atomic layer implies that the impurity or solute will exist in that layer. On the contrary, a positive value of a surface segregation energy E on an atomic layer implies that the impurity or solute cannot exist in that layer. Excepting Ni in Pt host, our calculated

Table 3. The segregation energies E_i (eV) of a single impurity to the ith atomic layer of a (1 0 0) surface. The segregation energy is the total energy of the host with a single impurity in the ith layer of a (1 0 0) surface relative to the energy of the impurity in the bulk of a host fcc metal. The columns correspond to the impurity and the rows correspond to the host, and the second column lists the (1 0 0) surface energies Q (mJ·m^{-2}) of the host metals [69].

			Impurity								
Host	Q	E_i	Cu	Ag	Au	Ni	Pd	Pt	Rh	Al	Ir
Cu	1651	E_1		−0.0701	−0.207	0.1061	−0.0555	0.2138	0.2754	−0.0917	0.3455
				−0.46 [41]	−0.40 [41]	0.11 [41]	−0.13 [41]	0.15 [41]			
					−0.37 [44]	0.233 [48]					
					−0.49 [45]						
				Y [42,43]	Y [46,47]	N [49]					
				−0.28 [67]	−0.14 [67]	0.12 [67]	−0.03 [67]	0.21 [67]	0.13 [67]		0.42 [67]
		E_2		−0.0038	−0.0448	−0.256	0.0194	0.072	−0.0117	0.0548	−0.0343
				−0.04 [41]	−0.01 [41]	−0.03 [41]	0.04 [41]	0.01 [41]			
						−0.147 [48]					
		E_3		−0.0031	−0.005	−0.0016	0.0038	0.0057	−0.0038	0.0047	−0.0043
		E_4		0.0001	−0.0001	0	0.0001	0.0001	−0.0001	0.0001	−0.0001
Ag	1275	E_1	0.1613		0.0505	0.328	0.0877	0.0189	0.7569	−0.1178	0.9434
			0.1 [41]		0.11 [41]	0.11 [41]	0.24 [41]	0.42 [41]			
			N [45]		N [50]						
			0.15 [67]		0.07 [67]	0.35 [67]	0.28 [68]	0.27 [67]	0.46 [67]		0.55 [68]
		E_2	−0.0192		0.0408	−0.0227	0.0285	−0.0737	−0.0685	0.0486	−0.1215
			−0.01 [41]		0.01 [41]	−0.03 [41]	0.02 [41]	−0.01 [41]			
		E_3	−0.0011		0.0022	−0.0011	0.0016	−0.0025	−0.0016	0.002	−0.0018
		E_4	0		0	0	0	0	0	0	0
Au	1083	E_1	0.4818	−0.1394		0.7025	0.2863	0.0877	1.1626	−0.0614	1.379
			0.15 [41]	−0.07 [41]		0.15 [41]	0.21 [41]	0.38 [41]			
			0.56 [44]								
			N [46,47]	Y [43,51]		N [52]	N [53]				
			0.34 [68]	−0.04 [67]		0.56 [68]	0.28 [68]	0.21 [67]	0.44 [68]		0.50 [68]

		E_2	−0.054	−0.0607		−0.0597	0.0827	−0.1651	−0.1347	0.122	−0.2101	
			−0.07 [41]	−0.03 [41]		−0.13 [41]	0.04 [41]	−0.05 [41]				
		E_3	−0.0231	−0.0036		−0.0025	0.0036	−0.0054	−0.0036	0.0045	−0.0041	
		E_4	0	0		0	0	−0.0001	0	0.0001	0	
Ni	2434	E_1	−0.1076	−0.067	−0.3047		−0.0114	−0.3002	0.0796	−0.1414	0.0728	
			−0.18 [41]	−0.75 [41]	−0.94 [41]		−0.62 [41]	−0.32 [41]				
			−0.426 [48]									
			Y [51,54]		Y [52,55,56]		Y [57]					
			−0.25 [67]	−0.58 [67]	−0.46 [67]		−0.27 [67]	−0.17 [68]	−0.10 [68]		0.16 [68]	
		E_2	0.0096	−0.005	−0.0445		0.0243	0.0721	−0.0249	0.0613	−0.0593	
			0.02 [41]	−0.03 [41]	−0.03 [41]		0.02 [41]	0.00 [41]				
			0.045 [48]									
		E_3	0.0021	−0.0054	−0.0071		0.0054	0.0079	−0.0054	0.0066	−0.0061	
		E_4	0	−0.0001	0		0.0001	0	−0.0001	0.0001	−0.0001	
Pd	1661	E_1	0.0783	−0.0922	−0.0991	0.2501		0.0371	0.584	−0.1585	0.7405	
			0.03 [41]	−0.25 [41]	−0.18 [41]	0.02 [41]		0.22 [41]				
				Y [58]	Y [53]	N [57,59]		N [60]				
			0.04 [68]	−0.26 [68]	−0.14 [67]	0.22 [67]		0.19 [68]	0.36 [68]		0.77 [67]	
		E_2	−0.0404	−0.0536	−0.0112	−0.0581		−0.018	−0.0965	−0.1038	−0.1592	
			−0.12 [41]	−0.15 [41]	−0.08 [41]	−0.19 [41]		−0.10 [41]				
		E_3	−0.002	−0.0052	−0.0069	−0.0021		−0.0046	−0.003	−0.0038	−0.0034	
		E_4	0	−0.0001	−0.0001	0		−0.0001	0	0	0	
Pt	2168	E_1	−0.4553	−0.0203	−0.0985	−0.7136	−0.1975		1.0925	−0.1615	1.2977	
			−0.04 [41]	−0.44 [41]	−0.49 [41]	−0.01 [41]	−0.23 [41]		0.966 [41]			
			Y [61,62]		Y [62]	N [63]	Y [60]		N [64,66]			
			0.32 [67]	−0.25 [67]	−0.32 [67]	0.46 [67]	−0.01 [67]		0.26 [68]		0.44 [67]	

Table 3. *Continued...*

Host	Q	E_i	Impurity									
			Cu	Ag	Au	Ni	Pd	Pt	Rh	Al	Ir
		E_2	−0.0867	−0.1075	0.1842	−0.1084	0.1272		−0.1802	0.1841	−0.2741
			−0.09 [41]	−0.06 [41]	0.04 [41]	−0.20 [41]	0.12 [41]				
		E_3	−0.0043	−0.0063	0.0082	−0.0045	0.0063		−0.0063	0.0077	−0.007
		E_4	−0.0001	−0.0001	0	−0.0001	0.0001		−0.0001	0.0001	−0.0001
Rh	2896	E_1	−0.7372	−0.5362	−0.2923	−0.5738	−0.5378	−0.1992		−0.443	0.227
				Y [65]				Y [66]			
			−0.41 [67]	−0.92 [67]	−0.82 [67]	−0.17 [67]	−0.47 [67]	−0.26 [67]			0.23 [68]
		E_2	0.0185	0.013	0.0388	0.037	0.0201	0.0501		0.0458	−0.0887
		E_3	0.0014	0.0036	0.0046	0.0014	0.002	0.0029		0.0043	−0.0022
		E_4	0	0.0001	0.0001	0	0	0		0.0001	0
Al	900	E_1	0.5029	0.1727	0.0598	0.7153	0.3168	0.1573	1.1279		1.3299
		E_2	−0.0327	−0.0249	−0.0567	−0.0378	−0.0442	−0.0872	−0.0937		−0.1594
		E_3	−0.0016	−0.0024	−0.0031	−0.0017	−0.0024	−0.0035	−0.0024		−0.0026
		E_4	0	0	0	0	0	0	0		0
Ir	2895		−1.0846	−0.8558	−0.5739	−0.9017	−0.8568	−0.4617	−0.2564	−0.7455	
		E_1	−0.18 [67]	−1.00 [68]	−1.12 [67]	0 [67]	−0.58 [67]	−0.57 [67]	−0.13 [67]		
		E_2	−0.0421	−0.0564	−0.091	−0.0617	−0.057	−0.0967	−0.0809	−0.0963	
		E_3	−0.0017	−0.0045	−0.0058	−0.0018	−0.0025	−0.0035	−0.0025	−0.0054	
		E_4	0	−0.0001	−0.0001	0	0	0	0	−0.0001	

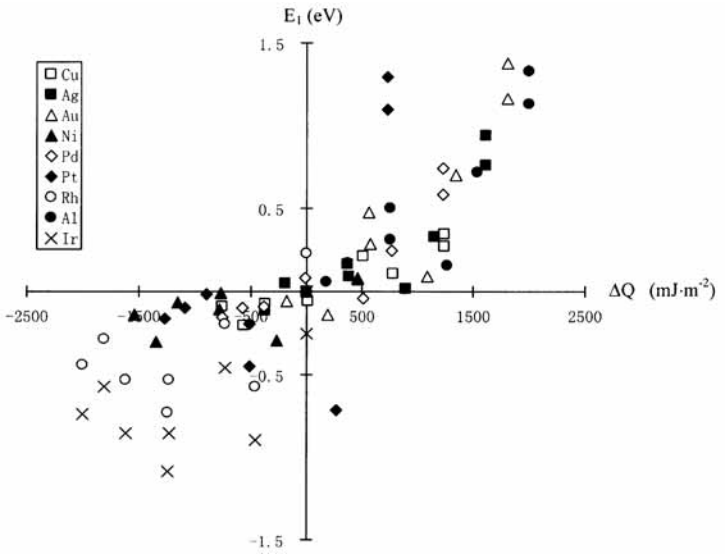

Figure 1. Relation between the segregation energy of the first layer E_1 (eV) and the differences in the (1 0 0) surface energy of the impurity to host crystals $\Delta Q = Q_{\text{imp}} - Q_{\text{hos}}$ (mJ·m^{-2}) for nine fcc metals Cu, Ag, Au, Ni, Pd, Pt, Rh, Al and Ir.

results are in good agreement with the available experimental results (table 3) with 'Y' representing the detected impurity in the surface and 'N' representing the undetected impurity in the surface. In spite of our calculated values of segregation energy not completely the same as other available theoretical results, the signs of the segregation energy are identical. In this article, the surface segregation energies of Rh and Ir are also calculated, which are not calculated in previous EAM calculation [41]. Most of our calculated values, for example, Pd and Pt in Cu, Cu, Au and Ni in Ag, Pd in Au, Rh in Ni, Ni and Ir in Pd and Ir in Rh, are closer to the first principle values [67,68] than that calculated by EAM. Unfortunately, there are no theoretical values that can be compared with Al.

An oscillatory damping phenomenon appears for a single impurity in each of the first four layers other than a monotonic damping for Ag, Au or Pt in Cu, Au or Pd in Ag, Ag or Pd in Au, Ag or Au in Ni, Ag, Au, Pt or Al in Pd, Cu, Ag or Ni in Pt, and eight impurities in Ir host. An oscillation in the segregation energy corresponds to an oscillation in the composition profile and a monotonic damping means a composition convergence to the bulk value monotonically. Furthermore, the absolute values of E_1 for a single impurity in the first layer is much higher than the absolute values of E_2, E_3 and E_4 for a single impurity in the second, third and fourth layer. The results show that the effect of the surface is down to the fourth-layer and an oscillatory or monotonic damping ($|E_1| > |E_2| > |E_3| > |E_4|$) phenomenon in segregation energy has been obtained. Such a damping phenomenon has also been observed in other calculations for E_1 and E_2 excepting Cu or Ni in Pd or Pt host, the segregation energies being larger for the second layer than for the first layer [41].

The absolute values of E_1 for a single impurity in the first layer is much higher than that in the nether layers. Thus, the surface segregation will work or not is mainly determined by the segregation energy of the first layer E_1. In order to explain the surface segregation phenomena, the relation between the segregation energy of the first layer E_1 and the differences in the (1 0 0) surface energy [69] of the impurity to host crystals $\Delta Q = Q_{\text{imp}} - Q_{\text{hos}}$ is illustrated in figure 1. It is interesting to note that 66 among 72 data points (excepting Au in Ag, Ag in Au, Cu or Pt in Pd, Ni in Pt and Ir in Rh host) drop to the first and third quadrants. That is, a positive (negative) segregation energy E_1 corresponds to a positive (negative) difference in the (1 0 0) surface energy between the impurity and host crystals ΔQ. Thus, we conclude that an impurity with lower surface energy will segregate to the surface of the host with higher surface energy. On the other hand, an impurity with higher surface energy cannot segregate to the surface of the host with higher surface energy. For example, the eight impurities (except Ir in Rh host) can segregate to the first layer of Rh or Ir host (1 0 0) surface since the surface energy of 2896 and 2895 mJ·m^{-2} for Rh and Ir respectively is higher than that of the other impurity metals. On the contrary, all eight impurities cannot segregate to the first layer of the Al host (1 0 0) surface since Al has the lowest surface energy (900 mJ·m^{-2}).

4. Conclusions

Segregation of the impurity or solute to the surface, interface, grain or phase boundary relates directly to many surface or interface phenomena. The surface segregation energies for a single impurity to the (1 0 0) surface have been calculated using the MAEAM for nine fcc metals (Cu, Ag, Au, Ni, Pd, Pt, Rh, Al and Ir). The lattice relaxation is treated with the molecular dynamics (MD) simulation at a temperature of absolute zero at constant volume. The simulation configurations have been iteratively computed based on the energy minimization principle. The effect of the surface is only down to the fourth-layer and an oscillatory or monotonic damping phenomenon in segregation energy has been observed. Examining the relation between the segregation energy E_1 for a single impurity in the first atomic layer and the differences in surface energy between the impurity and host crystals $\Delta Q = Q_{\text{imp}} - Q_{\text{hos}}$, we conclude that an impurity with lower surface energy will segregate to the surface of the host with higher surface energy.

Acknowledgements

The authors would like to acknowledge the State Key Development for Basic Research of China (Grant No. 2004CB619302), and the National Natural Science Foundation of China (Grant No. 50271038) for providing financial support for this research.

References

[1] K F McCarty, J A Nobel and N C Bartelt, *Nature (London)* **412**, 622 (2001)
[2] M J Rost, S B van Albada and J W M Frenken, *Surf. Sci.* **518**, 21 (2002)
[3] Y Gauthier, Y Joly and R Baudoing, *Phys. Rev.* **B31**, 6216 (1985)

[4] J L Rousset, A J Renouprez and A M Cadrot, *Phys. Rev.* **B58**, 2150 (1998)
[5] S E Hornstrom and L I Johansson, *Appl. Surf. Sci.* **27**, 235 (1986)
[6] M Ahmad and T T Tsong, *Appl. Phys. Lett.* **44**, 40 (1984)
[7] W T Geng, *Phys. Rev.* **B68**, 233402 (2003)
[8] L Fritschea and J Kollerb, *J. Solid State Chem.* **176**, 652 (2003)
[9] F R de Boer, R Boom, W C M Mattens, A R Miedema and A N Niessen, *Cohesion in metals* (Elsevier Science Publishers, Amsterdam, 1988) p. 84
[10] J R Chelikowsky, *Surf. Sci.* **139**, L197 (1984)
[11] P Lambin and J P Gaspard, *J. Phys.* **F10**, 2413 (1980)
[12] S Mukherjee and J L Moran-Lopez, *Surf. Sci.* **188**, L742 (1987)
[13] M Brejnak and P Modrak, *Surf. Sci.* **247**, 215 (1991)
[14] A F C Camposa, F A Tourinhoa, G J da Silvab and J Depeyrotb, *J. Magn. Magn. Mater.* **289**, 171 (2005)
[15] M S Daw, S M Foiles and M I Baskes, *Mater. Sci. Rep.* **9**, 251 (1993)
[16] M J Stott and E Zaremba, *Phys. Rev.* **B22**, 1564 (1980)
[17] J K Nørskov and N D Lang, *Phys. Rev.* **B21**, 2131 (1980)
[18] M S Daw and M I Baskes, *Phys. Rev. Lett.* **50**, 1285 (1983)
[19] M S Daw and M I Naskes, *Phys. Rev.* **B29**, 6443 (1984)
[20] A Landa, P Wynblatt, D J Siegel, J B Adams, O N Mryasov and X Y Liu, *Acta. Mater.* **48**, 1753 (2000)
[21] R A Johnson, *Phys. Rev.* **B37**, 3924 (1988)
[22] R A Johnson and D J Oh, *J. Mater. Res.* **4**, 1195 (1988)
[23] D J Oh and R A Johnson, *J. Mater. Res.* **3**, 471 (1988)
[24] B W Zhang, Y F Ouyang, S Z Liao and Z P Jin, *Phys.* **B26**, 218 (1999)
[25] B W Zhang, W Y Hu and X L Shu, *Theory of embedded atom method and its application to materials science* (Hunan University Press, Changsha, 2002)
[26] S M Foiles and M S Daw, *J. Mater. Res.* **2**, 971 (1987)
[27] R W Dickson and J B Wachtman, *J. Appl. Phys.* **40**, 2276 (1969)
[28] F Ma, J M Zhang and K W Xu, *Surf. Interface Anal.* **36**, 355 (2004)
[29] J M Zhang, X M Wei and H Xin, *Appl. Surf. Sci.* **243**, 1 (2005)
[30] J M Zhang, Y H Huang, X J Wu and K W Xu, *Appl. Surf. Sci.* **252**, 4936 (2006)
[31] J M Zhang, Y Shu and K W Xu, *Appl. Surf. Sci.* **252**, 5207 (2006)
[32] J M Zhang, X L Song, X J Zhang, K W Xu and V Ji, *Surf. Sci.* **600**, 1277 (2006)
[33] B W Zhang and Y F Ouyang, *Phys. Rev.* **B48**, 3022 (1993)
[34] W Y Hu, B W Zhang, X L Shu and B Y Huang, *J. Alloys Compd.* **287**, 159 (1999)
[35] J H Rose, J R Smith, F Guinea and J Ferante, *Phys. Rev.* **B29**, 2963 (1984)
[36] C S Barrett and T B Massalski, *Structure of metals* (Pergamon Press, Oxford, 1980)
[37] C Kittle, *Introduction to solid state physics* (Wiley, New York, 1976)
[38] R A Johnson, *Phys. Rev.* **B39**, 12554 (1989)
[39] D E Gray, *American institute of physics handbook* (McGraw-Hill Book Company, New York, 1972)
[40] R A Johnson, *Phys. Rev.* **B39**, 12544 (1989)
[41] S M Foiles, M I Baskes and M S Daw, *Phys. Rev.* **B33**, 7983 (1986)
[42] P Braun and W Faber, *Surf. Sci.* **57**, 57 (1976)
[43] B E Sundauist, *Acta. Metall.* **12**, 585 (1964)
[44] G Bozzolo, B Good and J Ferrante, *Surf. Sci.* **289**, 169 (1993)
[45] S Schomann and E Taglauer, *Surf. Rev. Lett.* **3**, 1823 (1996)
[46] J M McDavid and S C Fain, *Surf. Sci.* **52**, 161 (1975)
[47] H C Potter and J M Blakely, *J. Vac. Sci. Technol.* **12**, 635 (1975)
[48] S M Foiles, *Phys. Rev.* **B32**, 7685 (1985)

[49] K Watanabe, M Hashiba and T Yamashina, *Surf. Sci.* **61**, 483 (1976)
[50] S H Overbury and G A Somorjai, *Surf. Sci.* **55**, 209 (1976)
[51] G C Nelson, *J. Vac. Sci. Technol.* **13**, 512 (1976)
[52] P Wynblatt and R C Ku, *Surf. Sci.* **65**, 511 (1977)
[53] A Jablonski, S H Overbury and G A Somorjai, *Surf. Sci.* **65**, 578 (1977)
[54] M P Seah and C Lea, *Philos. Mag.* **31**, 627 (1975)
[55] J J Burton, C R Helms and R S Polizzotti, *J. Vac. Sci. Technol.* **13**, 204 (1976)
[56] J J Burton, C R Helms and R S Polizzotti, *J. Chem. Phys.* **65**, 1089 (1976)
[57] C T H Stoddart, R L Moss and D Pope, *Surf. Sci.* **53**, 241 (1975)
[58] B J Wood and H Wise, *Surf. Sci.* **52**, 151 (1975)
[59] K Wandelt and G Z Ertl, *Naturforsch.* **31**, 205 (1976)
[60] J du Plessis, G N van Wyk and E Taglauer, *Surf. Sci.* **220**, 381 (1989)
[61] J H Anderson, P J Conn and S G Brandenberger, *J. Catal.* **16**, 326 (1970)
[62] J A Schwartz, R S Polizzotti and J J Burton, *J. Vac. Sci. Technol.* **14**, 457 (1977)
[63] J J Burton and R S Polizzotti, *Surf. Sci.* **66**, 1 (1977)
[64] J Siera, van Delft FCMJM, A D van Langeveld and B E Nieuwenhuys, *Surf. Sci.* **264**, 435 (1992)
[65] J H Anderson, P J Conn and S G Brandenberger, *J. Catal.* **16**, 404 (1970)
[66] G C Williams and F Williams, in: *Proc. American Vacuum Society Meeting* (San Francisco, 1978)
[67] A Christensen, A V Ruban, P Stoltze, K W Jacobsen, H L Skriver, J K Nørskov and F Besenbacher, *Phys. Rev.* **B56**, 5822 (1997)
[68] A V Ruban, H L Skriver and J K Nørskov, *Phys. Rev.* **B59**, 15990 (1999)
[69] J M Zhang, F Ma and K W Xu, *Appl. Surf. Sci.* **229**, 34 (2004)